Journal

Numerical Analysis for the Determination of Stress Percolation in Dry-Stacked Wall Systems

S. AGAAJANI[1], D. WALDMANN[2], F. SCHOLZEN[2], A. LOUGE[3]
[1] *Civil Engineer, PhD, Luxembourg City, 1637 Luxembourg, shahriar.agaajani@asars.lu*
[2] *Professors, Faculty of Sciences, Technology and Communication, University of Luxembourg, Luxembourg City, 1359 Luxembourg, daniele.waldmann@uni.lu*
[3] *Mechanical Engineer, PhD, Luxembourg, alouge@pt.lu*

ABSTRACT
This paper comprises a portion of a PhD study concluding on the potential use of a new mortarless and modular masonry system by taking into consideration the outcome of a multidisciplinary study including aspects of experimental, numerical and analytical investigations in relation to a practical and economical development of modular load-bearing dry-stacked masonry systems. Different forms of interlocking masonry elements have been modelled and optimised thermo-mechanically. Full-scale masonry walls were assembled and tested experimentally under compressive, flexural, shear, cyclic and long term loads. The overall structural behaviour was compared to conventional masonry systems such as hollow and shuttering blocks. The investigations showed overall relative high structural performances for the developed dry-stacked elements. The effect of dry joint interfaces was extensively investigated experimentally and numerically under FE analysis. Based on the experimental observations, a numeric-analytical failure mechanism of the dry-stacked masonry structure is anticipated under axial and flexural loading. The structural investigations and engineering processes are completed by the development of a package of dry-stacked units consisting of interlocking modular masonries and an accompanying array of various other precast parts. This confirmed the practical issues and solutions towards the exploitation of the developed dry-stacked elements for the construction of ready-to-build, modular and load-bearing walls.

The portion of work presented herein proposes a new numerical technique for the determination of stress-distribution in dry stacked load-bearing structures. The model is developed in three steps under a numerical computing environment. First, based on geometrical properties of the dry-stacked elements and with a linear-elastic material behaviour, the load distribution and intensity in dry-stacked masonry walls is determined. In a second step, a phenomenon known as a plastic accommodation which accompanies the redistribution of the stress is incorporated in the model. This enables the understanding of the evolution of the stress distributions in the post-elastic phase, which is crucial for the determination of the load capacity and stability of the structure as a function of an increased external load. This paper also supports the better understanding of early fissuring in dry-stacked masonry structures which has an important influence on the overall stability of the structure. Finally, in a third step, the improvement of dry-stacked structures is pursued by further analysis of the results obtained through the algorithm.

This paper represents a new tool for investigating the localized and randomly defined internal stress distribution induced by external compression forces on dry-stacked structures. Furthermore, the algorithm illustrates that experimental investigations on dry-stacked systems may only give real indications on the load capacity of the structure, when the number of joint interfaces and height to length ratio of the block is based on actual sizes and that results of experimental investigations on reduced size prism specimens may not be extrapolated to full sized walls as they may over-evaluate the effective loaded masonry sections and therefore the overall load capacity.

KEYWORDS: masonry, dry-stacked, load distribution and intensity, strength, mortarless contact, modular block, load-bearing wall.

NOTATIONS

h	block or wall height
μ	mean value
σ	standard deviation
$[H]$	matrix H
h_{block}	block height
randperm(p)	returns a random value of the integers 1 to p
$[B]_{full}$ and $[B]_{half}$	individual full or half blocks
N_{ij}	node i,j
$[W]$	matrix W
α	alpha
L	length of wall
$A_{eff,i}$	effective loaded area Aeff,i at a given row i
k_i	reduction factor in row i
$A_{nom,i}$	nominal contact area in row i
n	number of cases
k_{min}	minimal reduction factor
$k_{min,env.}$	minimal envelope
Δh_{wall}	height difference in structures

1. INTRODUCTION

The understanding of structural behaviour of dry-stacked masonry systems implies defining load distribution, effective contact area at joint interface and determining the resulting stresses in the critical wall sections.

On the other hand, the production tolerances of dry-stacked masonry elements imply dimensional inaccuracies which have a substantial impact on the load-capacity and failure mode of the constructed walls. The effect of individual block height on stress distribution is investigated by developing a new technique in a numerical computing environment. This numerical investigation gives the relationship between the effective contact areas in a dry-stacked masonry wall as a function of the production tolerances and demonstrates that the contact area at the joint interface is under certain circumstances significantly lower than previously estimated. As a consequence, the better perception of the load distribution and intensity enables the development of post-elastic failure theories and masonry-shape improvement.

1.1 Load distribution in dry-stacked structures

As the mortared layers between the consecutive rows in a dry-stacked system are missing, the individual blocks must have exactly the same height for a uniform load distribution and transfer between the elements (Figure 1).

As a matter of fact, this ideal case is in reality not possible because of the production tolerances and dimensional inaccuracies, which induce a block-height distribution as indicated in Figure 2. These geometrical imperfections induce localized and almost unique internal stress distributions induced by external loads within the dry-stacked masonry wall.

Essentially the height differences between adjacent masonry elements, and marginally the variation of width of successive masonry rows for the block design shown in Figure 1 for example, have an impact on the load-capacity and failure mode of the constructed walls.

Past observations on load-bearing and dry-stacked masonry walls tried to analyse on how a dry-stacked masonry system responds to external loads. Although many experimental investigations have been undertaken in order to better understand the behaviour of these systems (Oh K., 1994) (Marzahn & König, 2002) (Drysdale, 2005) the load distribution within the walls have not been fully explained.

Transmission photoelasticity on stretcher-bond scale models have been used in tests, reproducing the load distribution of a locally applied vertical compressive force in photoelastic materials such as Plexiglas® (Bigoni, 2009). The results reveal localized, curvilinear stress distributions which do not diffuse as they would in a reinforced concrete system, but tend to distribute along high stiffness lines. Yet, a post-elastic approach such as cracking and its resulting consequences is not suggested.

This topic remains crucial for the understanding of stress distribution and intensity and is deepened within this research work by the development of a specific algorithm. The developed algorithm is based, initially, on a linear approach and thus no cracking of the elements is considered. In a second step, a post-elastic phase is considered by further examination of the sections with the highest stress concentrations.

1.2 Numerical setup and computing

By measuring the individual height of randomly selected blocks with a precision of 0.01mm, a frequency distribution may be obtained as a function of the height of the blocks (Figure 2), which serves to illustrate the geometrical imperfections. Although the distribution is slightly left-tailed (Table 1), the normal bell curve may be applied, and on account of its simplicity, is used as a first approximation:

$$f(h,\mu,\sigma) = \frac{1}{\sigma\sqrt{2\pi}} e^{-\frac{(h-\mu)^2}{2\sigma^2}} \quad (1)$$

The parameter h is the measured block height, μ is the mean value and σ the standard deviation of the distribution.

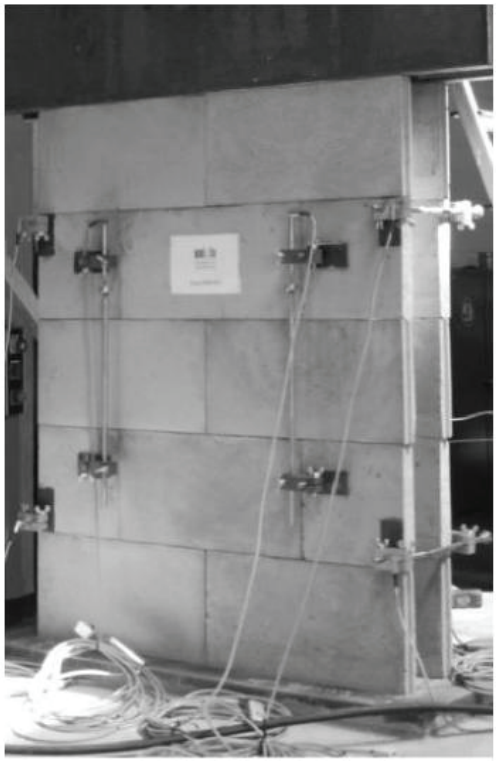

Figure 1 Dry-stacked masonry (Agaajani et al., 2015)

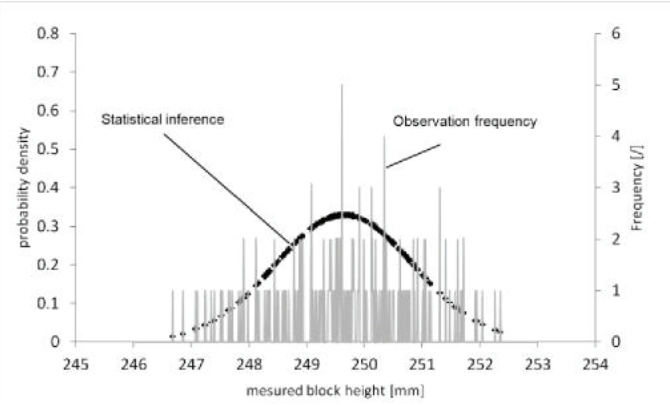

Figure 2 Normal distribution (black) and frequency (gray) of masonry height distribution of manufactured elements (Agaajani et al., 2015)

Figure 3 Definition of nodes of full and half masonry elements

Table 1
Statistical parameters (in mm) due to geometric imperfections in block production

Nominal height	Mean value	Median value	Standard deviation
250	249.64	249.62	1.20

Blocks with different heights (Equation (2)) are chosen randomly (Equation (3)) and stacked one by one until the desired height and length of the structure *[W]* is achieved (Equation (6) and Figure 4).

$$[H] = \begin{bmatrix} h_p = \mu - 3\sigma \\ \vdots \\ h_i = \mu \\ \vdots \\ h_1 = \mu + 3\sigma \end{bmatrix} \quad (2)$$

The matrix [H] contains empirical height measurements less than three standard deviations σ away from the mean value μ. For the discrete probability density function (Equation (1)) this accounts for 99.7% of the set. The randomly dry-stacked blocks are chosen using:

$$h_{block} = [H(randperm(p)] \quad (3)$$

Where h_{block} is the block height and [H] is a column matrix; randperm returns a random value of the integers 1 to p, where p is the size of the matrix [H].

Individual full blocks $[B]_{full}$ are modelled by 8 nodes (Equation (4)), whereas the half blocks $[B]_{half}$ are modelled by only 4 nodes (Equation (5)). The height difference between the upper and lower nodes is defined by Equation (3).

$$[B]_{full} = \begin{bmatrix} N_{21} & N_{22} & N_{23} & N_{24} \\ N_{11} & N_{12} & N_{13} & N_{14} \end{bmatrix} \quad (4)$$

$$[B]_{half} = \begin{bmatrix} N_{21} & N_{22} \\ N_{11} & N_{12} \end{bmatrix} \quad (5)$$

The "dry-stacking" of the masonry elements is achieved by incorporating the individual full and half masonry elements $[B]_{i,j}$ in a global matrix [W], which contains all the elements. The matrix [W], or wall, is constructed by placing the first row of elements on a perfectly horizontal line (corresponding to a mortared ground layer), and by placing the following rows in stretcher bond, for example. The ends of the structure are held laterally, which prohibits the rotation of the individual blocks. The load is applied uniformly on the upper and lower edges (Figure 4), while the dead load weight is omitted.

$$[W] = \begin{bmatrix} [B]_{1,j} & \cdots & [B]_{i,j} \\ \vdots & \ddots & \vdots \\ [B]_{1,1} & \cdots & [B]_{i,1} \end{bmatrix} \quad (6)$$

2. LOAD DISTRIBUTION AND INTENSITY

Figure 4 shows the example of a two-row wall structure, of 2.5mm length made of blocks with height variations corresponding to the frequency distribution of Table 1. The height difference between adjacent blocks is arbitrarily magnified for visualisation purposes (factor of 10). The load transmission from one row to another depends on the contact interfaces between the elements. The local rotation of the elements is not permitted and the horizontal gap between the elements is supposed to prohibit horizontal load transfer. Thus, it is assumed that forces distribute only vertically through the masonry rows.

The gap between two adjacent blocks causes the disruption of uniform load distribution which can be transmitted through the contact interface. As a consequence, the load is channelled through neighbouring contact interfaces, resulting in higher stress concentrations.

In Figure 5 two 2.5 x 2.5m wall structures are formed with all blocks except one of exactly the same height. In this first analysis, the block located in the middle of the lowest row is slightly higher than its neighbours. In the second case, the block with the higher height is located in the middle of the structure. In both cases, the block with the largest height tends to channel the load transmission by an angle α (angle taken from the vertical line of the load) above its location, which reduces the effective loaded area and induces high concentrations of stresses. It redistributes the load by the angle α, which may be given by:

$$\alpha = \tan^{-1}\left(\frac{\frac{L_{bloc}}{2}}{h_{bloc}}\right) \tag{7}$$

On the other side, a block with a reduced height induces a lack of contact between elements (Figure 6). The structure behaves as if there was an opening in the area around the element with the reduced height.

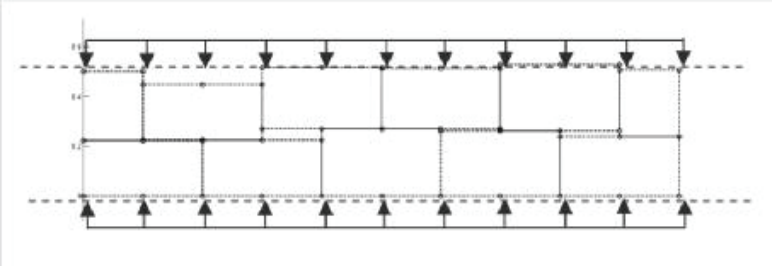

Figure 4 Randomly chosen blocks with different heights and dry-stacked in stretcher bond

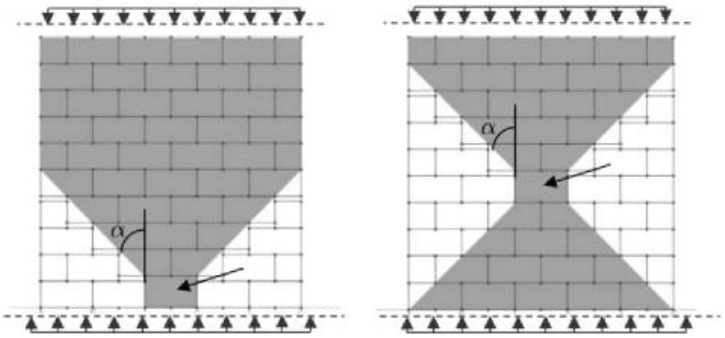

Figure 5 Visualisation of load-transmission in a dry-stacked wall structure using the above mentioned algorithm

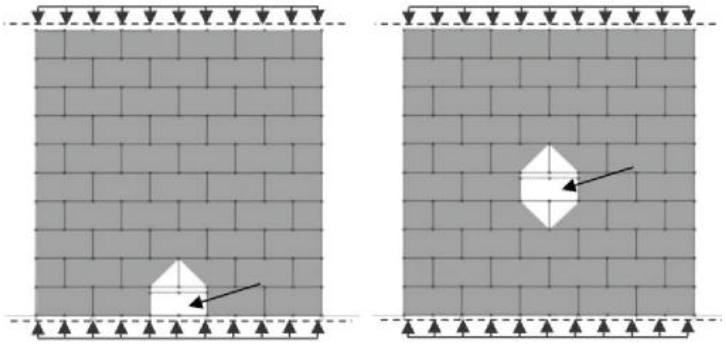

Figure 6 Influence of reduced block height on load transmission in dry-stacked wall systems

2.1 Load stress distribution in dry-stacked structures

Numerical simulations with randomly selected height values for every individual block show characteristic patterns of load distribution and transfer between the block elements in the structure. While the load is uniformly applied on the extremities of the wall, the effective area acting to transit load varies from row to row and decreases significantly to a minimum at the lower rows (Figures 7 and 8).

There are as many load percolations as stacking possibilities of randomly chosen blocks. Thus, we may state that the load percolation between each row is determined by a probabilistic state which is a function of the geometric properties of the used block population.

Generally, the load distribution varies throughout the height of the structure and is distributed through tree-like ramifications to the base, where only a small fraction of the total wall section is exploited. Note that the load distributions obtained do not take into consideration stress intensities.

The above mentioned observations show some analogy to numerical analysis and research of granular structures (Radjai, 1996) (Breton & Jussien), where the load transmissions through the more rigid structure is preferred and where curvilinear compressive stress lines occur (Figure 9).

Linear Finite Element analysis' models (Figure 10) validate the stress distribution in dry-stacked structures obtained through the developed algorithm. The results show virtually identical tree-like stress distributions, although the FEA may slightly better represent the stress in the different rows of the structure. However, the main added value in using the FEA, which are also time expensive (pre- and post-processing included), is the visualisation and determination of the developed stress intensity at the critical sections.

Figure 10 shows that for an external vertical load of 1MN/m^2 applied uniformly on each face-shell of the dry-stacked wall (Figure 1), the principal stress in the critical section of the structure may be 30 times higher than the least compressed sections (Agaajani et al., 2015). This additional numerical observation gives an insight into where initial cracking may occur and how the dry-stacked structures evolve in the post-elastic phase.

In Figure 11, where the length of the structure is a multiple of its height L > h, characteristic load distribution patterns are distinguished in comparison to the above mentioned structures (where h > L).

The global load transmission is improved, as the lower sections in the wall structure are better solicited through additional curvilinear compressive stress curves. Half-blocks are, if under compression, always entirely under compression, while full blocks are often only partially under compression. This observation elucidates why, in the running bond system, most of the full blocks and none of the half blocks were cracked on the load-bearing face shells during experimental loadings (Agaajani et al., 2015).

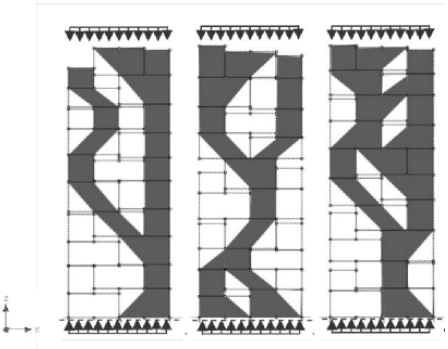

Figure 7 Load percolation in wall structures of 2.50m height and L = 1.00m length

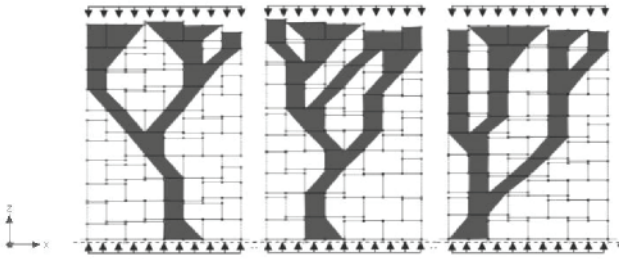

Figure 8 Load percolation in wall structures of 2.5m height and L = 2.00m length

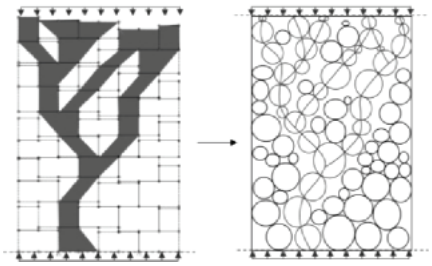

Figure 9 Analogy to granular structures

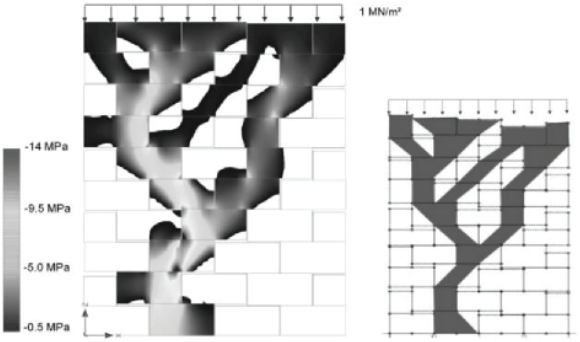

Figure 10 Stress percolation and intensity seen in a dry-stacked structure through FE Analysis (l.), compared to stress percolation obtained through the developed algorithm (r.)

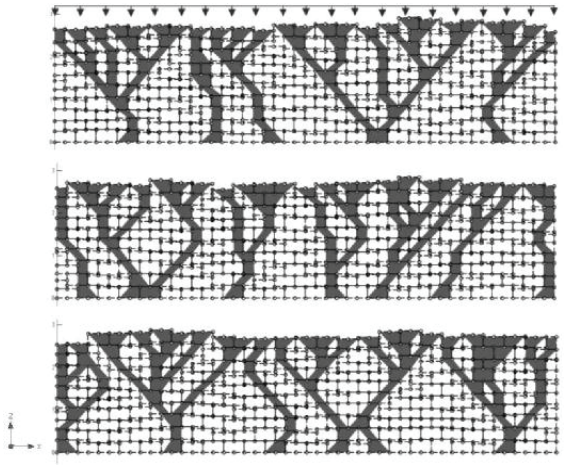

Figure 11 Vertical load transfer and distribution in a wall structure of ~2.5m height and length L = 12.00m with amplified standard deviation of 0.02m in height of randomly selected blocs (Agaajani et al., 2015)

2.2 Characteristic load intensities based on linear elastic behaviour

The effective loaded area $A_{eff,i}$ at a given row i in the masonry structure (Figure 12) is given by the relation:

$$A_{eff,i} = k_i \cdot A_{nom,i} \tag{8}$$

where k_i is a reduction factor of the loaded area at the contact interface between the rows i and i+1 due to the height differences between adjacent masonry elements, and $A_{nom,i}$ the nominal loaded area between the rows i and i+1.

The reduction factor k_i may be estimated by calculations based on statistical dispersions and geometric properties of individual block elements:

$$k_i = \frac{\sum_{c=1}^{n} \frac{A_{eff,i}}{A_{nom,i}}}{n} \tag{9}$$

Where n is the total number of analysed cases c in order to obtain an average value based on statistical dispersions and load distributions, for a given structure of height h and length L.

The existence of a minimal effective contact area $A_{eff,min,wall}$ is determined analytically in every dry-stacked structure and is defined by the geometrical properties of the individual block elements and of the entire structure:

$$k_{min} = \frac{1}{2} \cdot max\left(\frac{h_{block}}{h}; \frac{L_{block}}{L}\right) \tag{10}$$

Where, L_{block} and h_{block} are the length, andheight of a single block, and L and h are the length, and height of the entire dry-stacked structure.

As a result, locally concentrated forces cause premature cracking in the dry-stacked masonry elements and reduce the overall elastic behaviour and load-bearing capacities of the wall.

In Figure 13 the statistically determined evolution of the reduction coefficient of the loaded area, for a 2.5m high structure and varying lengths is shown. This reduction coefficient retraces for each row the relation between the effective loaded area due to imperfections and the theoretical global total area depending on different wall lengths (from L = 0.25m to L = 12m). The minimum envelope, the heavy black line (Equation (11)), representing an endless length of wall shows a drastic reduction of the loaded area in the lower part of the masonry structure (reduction of 80-90% at the four lowest courses of the masonry). The test results of Jaafar et al. (2006), where large differences in normal displacements at joint interfaces were measured at different locations, show during experiments the same behaviour: the crushing at joint interface was higher in the lower rows than the upper ones.

The statistically determined minimum reduction factor k_{min_env} is "approached" numerically by non-linear curve fitting and represented by Equation (11):

$$k_{min\_env.} = 0.12 + 0.05h^2 + 0.0011e^{h^2}$$
$$for\ h \in [0.25, 2.50m] \tag{11}$$

The column-wall formed with dry-stacked half blocks (L = 0.25m) does not have any adjacent neighbouring blocks with different heights, and therefore has a reduction coefficient equal to 1 over the entire height of the wall. For running-bonded structures of L = 0.5m and more, the distribution frequency (Figure 2) plays an important role and the reduction coefficient is drastically decreased as a function of a growing length of wall and position of the contact interface in the structure (Figure 13). For any h/L ratio, the poorest contact interface between the dry-stacked rows is reached on the interfaces of the lowest rows. This is a very important observation as it may demonstrate where initial cracking may occur. Furthermore, Figure 13 is obtained for a fixed height of 2.5m and variable lengths of dry-stacked system. Additional simulations for alternative wall heights would give more details about the reduction coefficient k_i.

2.3 Deviation of global height in dry-stacked structures

The random and non-linear difference in wall height between a dry-stacked structure, where all block elements have the same height, and a structure composed of blocks with a given standard deviation of their height corresponding to the actual production series (Table 1 and Equation (1)), is analytically given by the relation (12):

$$\Delta h_{wall} = 0.6h^2 + 2.9h + 1.7 \quad [mm]$$
$$for\ h \in [0.25, 2.50m] \tag{12}$$

In the particular case (standard deviation of 1.2mm), a desired structure of 2.5m height would be statistically ~13mm higher (~0.5%).

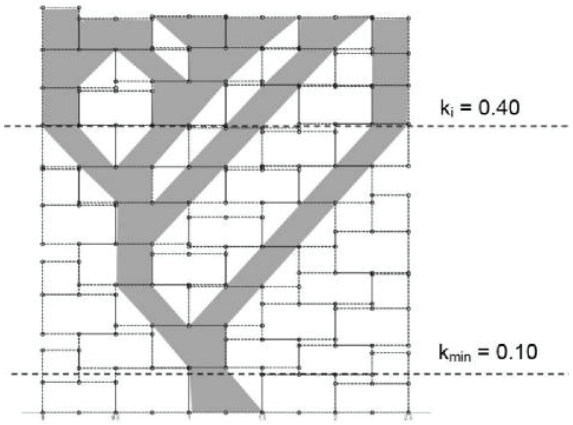

Figure 12 Example of effective area calculation for the determination of the stress state in dry-stacked masonry

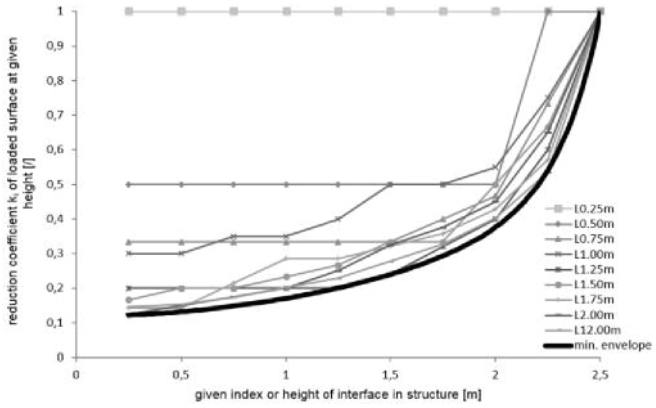

Figure13 Evolution of the reduction coefficient of loaded surface area

3. POST-ELASTIC PHASES IN DRY-STACKED MASONRY SYSTEMS

According to the previous observations, the understanding of stress distribution within dry-stacked masonry walls is found to be complex. The load distribution between the dry-stacked rows is being dominated by randomness and tree-like geometrical schemes with some analogy to granular mediums (Figure 9). Stress distribution is highly localized in the lower rows, highlighting stress columns in contrast to unloaded areas in the dry-stacked masonry walls. The evolution of these structures in the post-elastic phase with the associated stress and crack development are crucial for the determination of the load capacity and stability of these structures.

The analysis of block height distribution may enable the understanding of load distribution and intensity of load transfer at contact interfaces of dry-stacked masonry structures. According to experiments carried out at the University of Luxembourg (Agaajani et al., 2015), a 1m long and 2.5m high dry-stacked wall is modelled in stretcher-bond (Figure 14) and a uniform load is applied at the top of the structure. It is again supposed that the lateral edges of the structure are pinned, which prohibits the rotation of the individual blocks. In the analysis the load is applied uniformly at the top and bottom of the structure while the dead load weight is neglected.

An expected tree-like stress distribution pattern is observed, as described in the previous sections. In accordance with the reduction of the loaded surface area as a function of the position of the joint interface in the dry-stacked wall structure (Figure 15), the possible location of the critical wall section is found to be in the second row. The applied vertical load is then gradually increased, in order to initiate damage or cracking of the critical section (Figure 15, left side). Due to cracking of the critical element in the critical section, the concerned block is split in two parts, inducing a redistribution of stress in the dry-stacked system which is illustrated in the right side of Figure 15.

By further increasing the intensity of the applied vertical force, the next possible critical section is subjected to damage (Figure 15, right), and again, a new load and stress distribution is initiated as a result of this rearrangement of dry-stacked blocks in the dry-stacked wall (Figure 16, left). The rearrangement of the blocks and their changing stress distribution is pursued with the increase of the applied load (Figure 16, right).

In contrast to traditional masonry wall constructions, where damage initiation only appears close to the ultimate load and is thus a sign of reaching the load bearing capacity, the dry-stacked systems, due to cracking, enter state a more homogenous stress distribution with enhanced load distribution changes due to increased effective contact areas at joint interfaces (Figure 17, left). The stability of the damaged dry-stacked wall is also enhanced compared to the un-cracked situation, in spite of the cracked block elements, as the stress streams are more uniformly distributed and there are fewer unloaded areas. This phenomenon is known as plastic accommodation which accompanies the redistribution of the stresses.

If the load is continuously increased, without consideration to the slenderness of the wall, all the full elements may be divided into two half blocks, transforming the stretcher-bond system into a stack-bond system where the masonry elements are aligned vertically. The wall would be transformed into individual pillars (Figure 16, right), implying the highest rate of effective contact area between adjacent rows in the dry-stacked system. Due to a possible lateral mechanical interlocking of the adjacent masonry elements, the different pillars may not be fully independent.

The splitting of the full blocks due to cracking, starting at the lower rows of the wall with an increasing vertical loading has systematically been observed during experimental investigations on stretcher-bonded, dry-stacked masonry walls (Figure 18) (Agaajani Shahriar et al., 2015). Indeed, the cracking of the blocks appeared long before the ultimate load was reached. This proves the reorganisation of the stress distribution and reduction of stress intensity which takes place during the loading of the dry-stacked wall, as the wall changes into a series of columns.

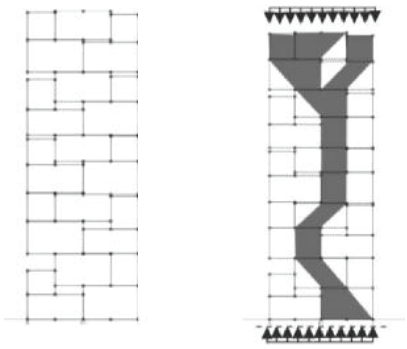

Figure14 Numerical modelling of a 1.0 x 2.5m dry-stacked wall (height differences between adjacent elements exaggerated for visualisation purposes)

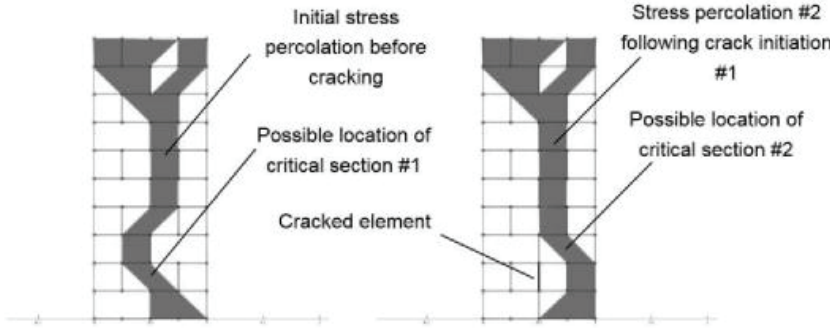

Figure 15 Comparison between initial stress distribution (left) and new stress distribution after cracking of the critical section #1 (right)

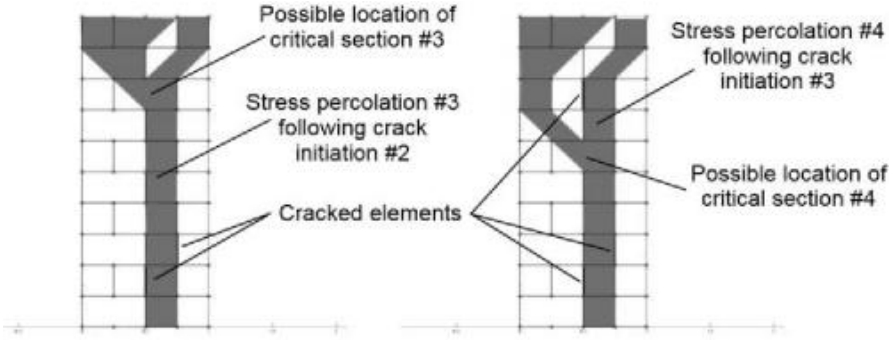

Figure 16 Comparison between initial stress distribution (left) and new stress distribution after cracking of the critical section #1 (right)

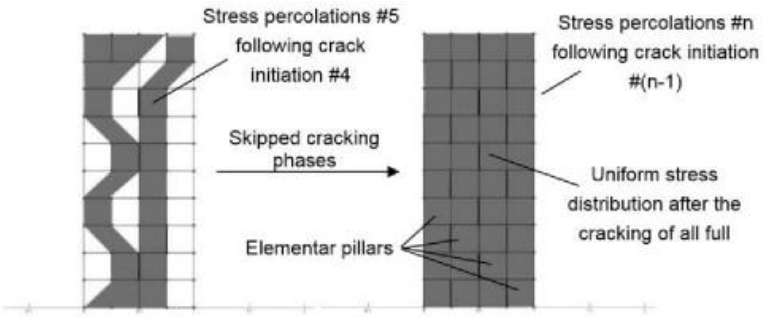

Figure 17 Comparison between stress distribution #5 (left) and final stress distribution #n after the cracking of all full block elements (right)

Figure 18 Characteristic crack patterns observed during experimental investigations involving vertical loadings and bending moments on stretcher-bonded and dry-stacked masonry structures

5. IMPROVEMENT OF THE LOAD CARRYING BEHAVIOUR

Repeating the same procedures and analysis with an increased block height of 0.5m, the load distribution through the dry-stacked masonry structure is modified and improved. Comparing Figures 8 and 11 and Figures 19 and 20, we notice that with the overall increased height of the elements, the load intensity through the structure is enhanced and as a consequence, the load distribution is improved, involving a reduction of stress intensity at a given height in the structure.

The maximum angle α of load transmission from one row to another is given by Equation (7) and is plotted as a function of the ratio of the block height to block length in Figure 21. We notice that for a more uniform load transmission it is necessary to reduce the angle α of load transmission in order to get more curvilinear stress lines, or an increased number of tree-like ramifications, in a given structure. To reduce the angle of load transmission which means to reduce the inclination of the stress lines towards the vertical, the ratio of the height to the length of the blocks must be increased for a given block length.

An increased block height (0.5m instead of 0.25m) for a given block length of 0.5m enhances the reduction factor k_i significantly which can be seen in Figures 22 and 23. As the number of intermediate joint interfaces is decreased from 9 to 4, there are less “disconnected contact layers”, and thus the load transmission is enhanced. We notice that the effective contact area at the lowest joint interface is increased by about 100%.

In comparison to Equation (11), the reduction coefficient k_i at a given joint interface or height h in the improved structure (h/L = 1.0) is given by the approximate curve-fitted relation (12) and is plotted in Figure 23:

$$k_{i,\min\_envelope} = 0.25 + 0.0024 \cdot 10^{h}$$
$$for\ h \in [0.50, 2.50m] \quad (12)$$

We may therefore postulate that the global structural behaviour of a dry-stacked wall is significantly improved when elementary blocks have a height-to-length ratio of 1.0. The ratio of 1.0 may be best practice as further restrictions such as block weight and manoeuvrability also play a significant role.

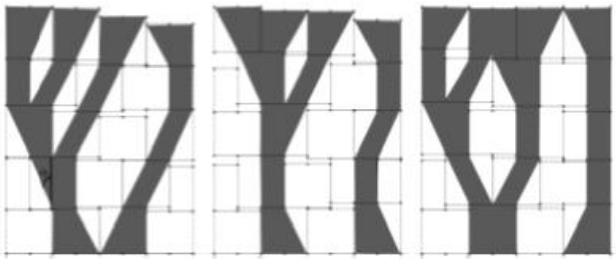

Figure 19 Load distribution in 2.00 m long and 2.5m height structures

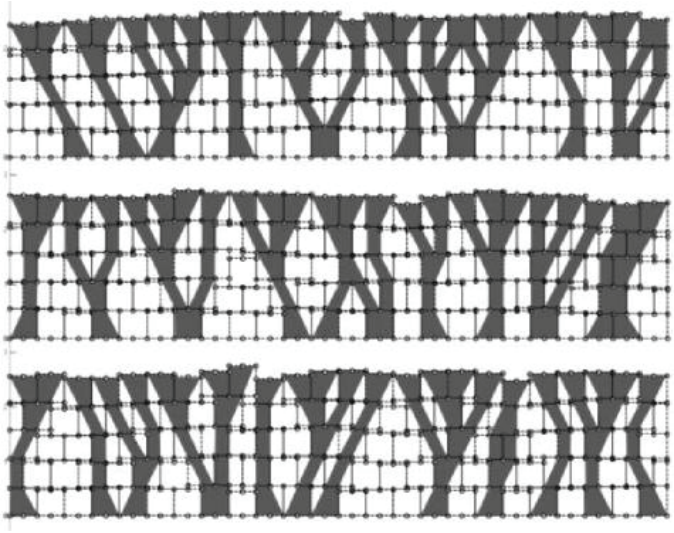

Figure 20 Wall structures of 2.5m height and L = 12.00m length

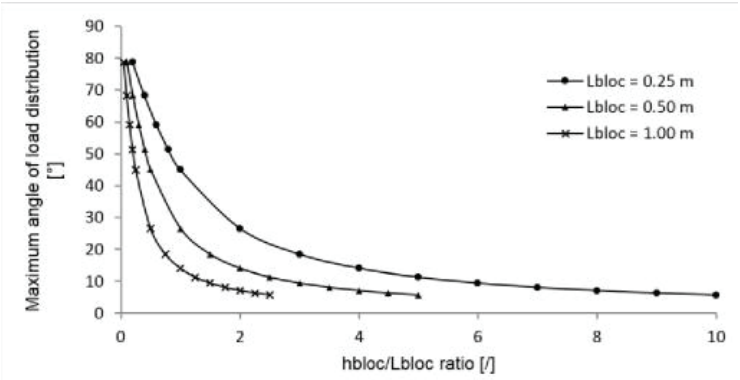

Figure 21 Maximum angle α of load transmission in function of h/L ratio of the masonry elements

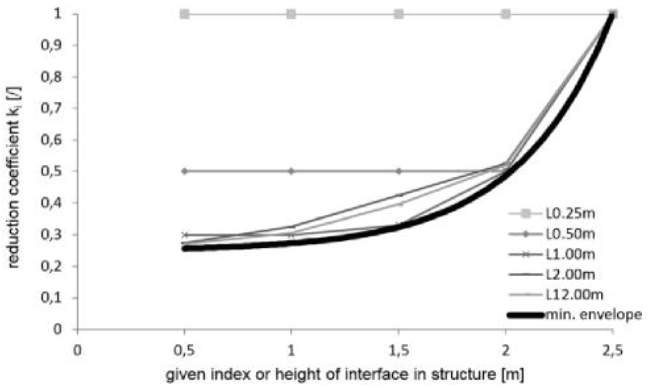

Figure 22 Reduction coefficient and minimum envelope of loaded area at a given index or height in dry-stacked structure of 2.5m height and for different lengths (n=5)

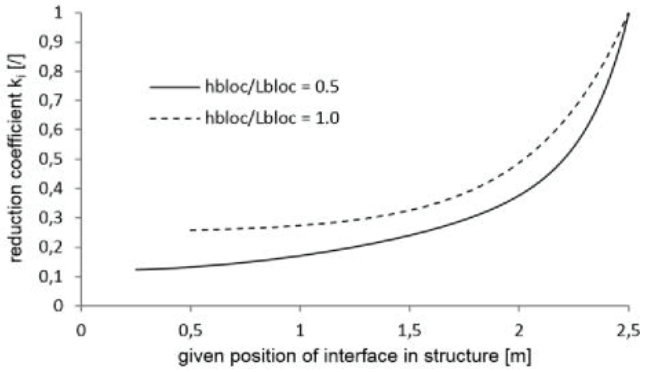

Figure 23 Comparison of reduction coefficient k_i for different h/L ratios of block elements

6. CONCLUSIONS

This work contributes to the field of dry-stacked masonry blocks with respect to load distribution in dry-stacked structures and post-elastic failure theories. The definition of the average contact area at joint interface between dry-stacked masonry elements in stretcher bond is highly complex. The effective area acting in the load transmission varies from row to row and decreases significantly to a minimum at the lowest rows. This first reduction coefficient, due to the height variation in block production is dependent on the block dimensions, and improves when the height to length ratio of the elements is increased.

This observation is crucial for the understanding of stress and crack development in dry-stacked masonry structures. Under the condition that all the contact interfaces behave similarly, the rows with the highest stress rates may crack first, in order to allow reorganisation of load transfer in the post-elastic phase. The evolution of stress distribution in the post-elastic phase is crucial for the determination of the load capacity and stability of the structure. Examination of the algorithm indicates how dry-stacked wall structures evolve under an increasing vertical force and represents a new tool for investigating the localized and randomly defined internal stress distribution induced by external compression forces.

The shape of the mortarless masonry element may be optimised for higher structural load capacity by having a unit height-to-length ratio of 1.0. The ratio of 1.0 would be best practice as further restrictions such as block weight and manoeuvrability play a significant role.

Furthermore, the simulations showed the importance of the global height of the dry-stacked masonry wall. In fact, any added dry-stacked row in the structure implies a decrease of the effective contact area and thus, increases the stress intensity at the joint interfaces. It may be concluded that experimental investigations on dry-stacked systems may only give real indications on the load capacity of the structure, when the number of joint interfaces and h/L ratio of the block is in accordance with actual materials: results of experimental investigations on reduced prism specimens may not be extrapolated to full sized walls as they may over-evaluate the load capacity.

REFERENCES

1. AGAAJANI, S., WALDMANN, D., SCHOLZEN, F., LOUGE, A. *Development and investigation of a new dry-stacked wall system*, PhD thesis, University of Luxembourg, 2015.
2. OH, K. Development and Investigation of Failure Mechanism of Interlocking Mortarless Masonry System, Philadelphia: Drexel University, 1994.
3. MARZAHN, G., & KÖNIG, G. Experimental Investigation of Long-Term Behaviour of Dry-Stacked Masonry. TMS Journal, 9-21, 2002.
4. DRYSDALE. Properties of Azar Dry-Stack Block IV Construction. Ontario: Azar Group Companies, 2005.
5. BIGONI, D. Localized stress percolation through dry masonry walls. Part I – Experiments, European Journal of Mechanics A/ Solids **29**, 291-298, 2009.
6. BIGONI, D. (2009). Localized stress percolation through dry masonry walls. Part II – Modelling, European Journal of Mechanics A/Solids **29**, 299-307, 2009.
7. RADJAI, F. Force distributions in dense two-dimensional granular systems, Physical review letters, 274, 1996.
8. BRETON, L. & JUSSIEN, N. Un CSP comme comportement d'agent. Application à la résolution d'équations en physique des milieux granulaires. LINA; Ecole des Mines de Nantes.
9. JAAFAR et al., ALWATHAF, THANOON, NOORZAEI, & ABDULKADIR. Behaviour of interlocking mortarless block masonry. Proceedings of the Institution of Civil Engineers - Construction Materials **159** (CM3), 111-117, 2006.
10. ABDULLAH et al. Structural Behaviour of a Mortarless Interlocking Blockwork System. Masonry International, Proceedings of conferences 2007 (pp. 527-532). Universiti Teknologi Malaysia: British Masonry Society, 1995.
11. CERVENKA, V., JENDELE, L. & CERVENKA, J. ATENA Program documentation Part 1 – Theory. Prague, 2010.
12. EDWARDS J. et al. Design and Construction of interlocking mortarless block masonry. Alberta: Department of Civil Engineering and Environmental Engineering, University of Alberta, 2010.
13. GAVRIEL, S. Handbook of human factors and ergonomics. New York: Wiley, 2006.
14. RAMAMURTHY and ANAND. Development and performance evaluation of interlocking-block masonry. Journal of architectural Engineering, 6:45- 51, 2000.
15. THANOON, J. Development of an innovative interlocking load bearing hollow block system in Malaysia. Elsevier Construction and Building Materials, pp. 445-454, 2004.